

# Fiber structure and properties of poly(ethylene-2,6-naphthalate) obtained by high-speed melt spinning

Gang Wu<sup>a,\*</sup>, Qingchun Li<sup>a</sup>, J.A. Cuculo<sup>b</sup>

<sup>a</sup>College of Material Science and Engineering, Beijing University of Chemical Technology, Box. 52, Beijing 100029, People's Republic of China

<sup>b</sup>Fiber and Polymer Science Program, College of Textiles, North Carolina State University, Raleigh, NC 27695-8301, USA

Received 11 January 2000; accepted 13 January 2000

## Abstract

High molecular weight poly(ethylene-2,6-naphthalate)(PEN) has been melt spun at various take-up velocities from 0.9 to 10 km/min to prepare fiber samples. The effect of take-up velocity on the structure and properties of as-spun fibers has been characterized through measurements of birefringence, density, wide-angle X-ray diffraction, infrared analysis, DSC melting behavior, tensile properties and high-temperature shrinkage. With increasing take-up speed, a steady trend toward higher as-spun fiber orientation and crystallinity was observed, accompanied by improved physical properties. The WAXD patterns of the as-spun fibers prepared at a velocity range higher than 1.5 km/min indicate that these samples all possess a developed molecular orientation and crystalline structure. At a relatively low take-up velocity that range from 1.5 to 4 km/min, a high level of molecular orientation in both crystalline and amorphous region has been found. This may be attributed to the high spinning stress generated by the high-molecular weight polymer used. In the high take-up speed region of 5–10 km/min, the molecular orientation becomes saturated. The highest tenacity and initial modulus of the as-spun PEN fibers obtained in this region reached ca 8 and 200 g/d, respectively. © 2000 Elsevier Science Ltd. All rights reserved.

**Keywords:** Poly(ethylene-2,6-naphthalate); High-speed melt spinning; Threadline tension

## 1. Introduction

The first report on poly(ethylene-2,6-naphthalate) (PEN) appeared in the literature dating back to 1948 by Cook et al. who described the synthesis method of this new aromatic polyester in which the benzene ring in poly(ethylene terephthalate) (PET) is replaced by a naphthalene ring [1]. Although its history is relatively long, only a few papers [2–6] had been published on structural studies of PEN until the 1980s. Increasing interest appears from the late 1980s [7–21], probably due to the boom of the so-called “high performance polymers” where PEN is considered to be a prime contender with its excellent mechanical properties and thermal stability [3,7,12,22]. The crystal structure of PEN was determined by Mencik [2] and Buchner et al. [9] Two crystal modifications, i.e.  $\alpha$  and  $\beta$  forms have been reported and both were found to be triclinic. The unit cell parameters of the  $\alpha$  form are  $a = 0.651$  nm,  $b = 0.575$  nm,  $c = 1.32$  nm,  $\alpha = 81.3^\circ$ ,  $\beta = 144^\circ$ ,  $\gamma = 100^\circ$ . The unit cell dimensions of the  $\beta$  form are  $a = 0.926$  nm,  $b = 1.559$  nm,  $c = 1.273$  nm, with angles of  $\alpha = 121.6^\circ$ ,  $\beta = 95.57^\circ$  and  $\gamma = 122.52^\circ$ .

Following a publication that has compared infrared spectra of PEN and PET, and assigned most vibrational bands in the spectrum of PEN [5], FTIR analysis has been used to study the neck formation and melting behavior for various samples with different drawing and heat treatment history [17,19]. A detailed thermal analysis of amorphous and various semicrystalline PEN samples has been reported several years ago [7], where the equilibrium melting parameters were reported to be  $T_m^0 = 337^\circ\text{C}$ ,  $\Delta H_f = 25 \pm 2.0$  kJ/mol and  $\Delta S_f = 41 \pm 3.3$  J/(kmol). Structural development during uniaxial drawing has also been studied [11,17]. Time-resolved two-dimensional wide-angle X-ray diffraction patterns are recorded using the imaging plate system for following the change of chain orientation in a disoriented amorphous film in the drawing process to help establish the mechanism of oriented crystallization of PEN [15,21].

Along with these studies of the structural features of PEN, there have been relatively fewer experimental studies of PEN spun fibers. Before the 1990s, only one investigation of high-speed melt spun PEN fiber was reported [4]. In the 1990s, several researchers published findings on the development of structure as a function of spinning speed and/or heat treatment of PEN. Iizuka and co-workers reported the

\* Corresponding author.

E-mail address: wug@public.bta.net.cn (G. Wu).

neck-like deformation behavior during the high-speed spinning of PEN using on-line profile measurement [23]. Nagai and Cakmak, respectively, reported their characterization results for as-spun and draw PEN yarns including fiber properties and crystal modifications [24–26]. Jager et al. prepared high-molecular weight PEN via the condensation polymerization route and compared the properties of the resultant PEN filament with those of PET industrial yarns [18]. In most of these articles, however, the take-up velocities were limited to 4–5 km/min. An exception was reported in 1997. Miyata et al. [27] reported the high-speed melt spinning of PEN at take-up velocities up to 9 km/min. In their study, however, raw material with relatively low-molecular weight was used.

In this article, melt spinning of PEN fiber was done over a wide take-up speed range between 0.9 and 10 km/min. Because a high-molecular weight polymer was used in this study, it is expected that the structural features may differ somewhat from those previously reported. Therefore, the effect of spinning conditions on the structural and physical properties of this high-molecular weight as-spun PEN fiber was studied.

## 2. Experimental

### 2.1. Materials

The PEN polymer used in this study was produced originally by condensation polymerization and then subjected to solid state polymerization to raise the molecular weight further. Intrinsic viscosity (IV) of polymer chip measured in a 60/40 (wt%) mixture of phenol and tetrachloroethane is 0.89 dl/g. This value, however, is believed to be slightly lower than the true value of the raw material, because the chips were subjected to a melting and quenching process prior to solution preparation, because of their high crystallinity. PEN chips were dried in a vacuum oven at absolute pressure of 0.1 mmHg at 140°C for 16 h before use.

### 2.2. Fiber spinning

PEN chip was processed in an extruder with a screw diameter of 25 mm and a length to diameter ratio of 25. A round single-hole spinneret having 0.6 mm diameter was used together with a throughput/wind-up speed arrangement to produce approximately 4.5 denier as-spun filament. Spinning temperature ranging from 310 to 320°C, and spinline length, between the spinneret face and take-up godet, varying from 2.6 to 4.4 m were tried to examine their respective influence on the spinnability and properties of the resultant fiber samples. Unless otherwise mentioned, however, a temperature of 310°C, and a spinline length of 4.4 m were used in most experiments. A heated sleeve 5 cm long was installed surrounding the spinneret face. It was maintained at 300°C. No cross-flow or radial quench chamber was used. After passing through the atmospheric medium, the filament

was collected on the godet at speeds varying from 0.9 to 10 km/min.

### 2.3. Measurements

Fiber denier was determined by the vibroscope method in accordance with ASTM D1577. The linear density of the sample expressed in g/cm was calculated using the following relation:

$$g/cm = t/(4L^2f^2) \quad (1)$$

where  $t$  is the fiber tension,  $L$  the effective fiber length, and  $f$  the fundamental resonant frequency.

Threadline tension was measured using a tensiometer manufactured by Tensiometrics, at a point near the take-up godet where the solidification is certainly complete, and the threadline diameter should have attained its final value. The threadline stress, therefore, was calculated simply by dividing the measured tension by the fiber denier.

Density of the fiber samples was measured following ASTM D1505-68. The density gradient column consisted of aqueous sodium bromine (NaBr) maintained at  $23 \pm 0.1^\circ\text{C}$ . An average value of three tests per sample was reported.

Birefringence measurements were made with a Leitz 20-order tilting compensator mounted in a Nikon polarizing microscope. An average of 10 individual determinations was reported.

Wide-angle X-ray diffraction (WAXD) measurements were performed on a Siemens type-F diffractometer system with  $\text{CuK}_\alpha$  radiation generated at 30 kV and 20 mA. The diffracting intensities were recorded every  $0.05^\circ$  from  $2\theta$  scans in the range  $5\text{--}40^\circ$ . WAXD photographs were recorded by a vacuum flat camera.

The structural characteristics of fibers were also examined by infrared spectroscopy. The unpolarized infrared absorption spectra were recorded with a Nicolet 510P spectrophotometer. Fiber samples were carefully arranged in a parallel pattern on a small metal frame so as to reduce the presence of air gaps or overlaps. All spectra were obtained at  $2\text{ cm}^{-1}$  resolution and averaged over 128 scans.

A Perkin–Elmer DSC-7 system was used for the thermal analysis of the PEN fibers. DSC scans were obtained during the first heating at a thermal scan rate of  $20^\circ\text{C}/\text{min}$ . The sample weights were kept between 8 and 10 mg. The calibration of melting temperature was made with a standard indium sample.

Mechanical properties of as-spun fibers were measured on an Instron tensile tester model 1122 at room temperature. All tests were performed using a gage length of 25.4 mm and a constant cross-head speed of 20 mm/min. An average of 10 individual tensile determinations was reported for each sample.

Hot air shrinkage (HAS) tests were performed following ASTM D4974-89. Initial length of the fibers was measured after applying a small pretension (0.1 g/d). Fiber sample

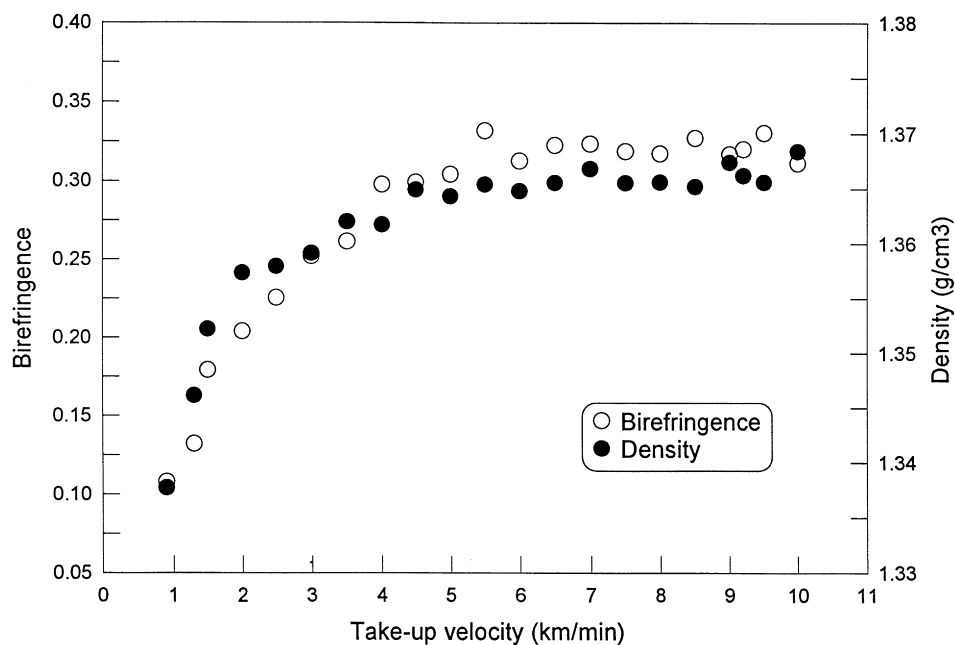


Fig. 1. Birefringence and density of as-spun PEN fibers as a function of take-up velocity.

was placed in an oven at 177°C for 5 min. After free shrinkage occurred, the samples were removed from the oven and the final length was measured. Shrinkage was then calculated using the following formula:

$$\text{Shrinkage} = [(L_i - L_f)/L_i] \times 100\% \quad (2)$$

where,  $L_i$  and  $L_f$  are the lengths of the fiber before and after shrinkage, respectively.

### 3. Results and discussion

#### 3.1. Structural changes of fiber sample

The structural development of the PEN fibers with increasing take-up velocities was followed by measurement of the birefringence and density of the as-spun products. The results are shown in Fig. 1. The birefringence values of the

fiber samples obtained over the entire range of take-up speeds are much higher than those of PET melt spun fibers spun under corresponding conditions. For PEN, the birefringence values vary from ca 0.1 to 0.3 in the take-up velocity range of 0.9–10 km/min, comparable values for typically spun PET filaments change at a lower level from 0.01 to 0.11 in the same take-up range [28]. This is attributed to higher intrinsic birefringence of PEN. By correlating polarized Raman spectroscopic data and birefringence measurements, an intrinsic birefringence value of 0.487 has been obtained for PEN and a value of 0.244 for PET [13]. As shown in Fig. 1, with increasing take-up velocity from 0.9 to 4 km/min, birefringence increases rapidly and reaches a value of ca 0.30, implying that an intensive development of molecular orientation occurs in the velocity range below 4 km/min. The birefringence tends to saturate in the speed range of 5–10 km/min at a level of  $\Delta n = 0.32$ . The overall density data as a function of take-up velocity are also

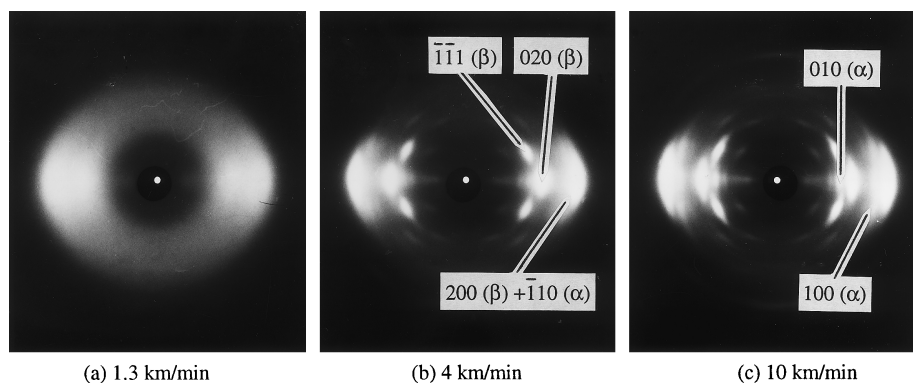


Fig. 2. WAXD photographs of as-spun PEN fibers taken-up at the indicated velocities.

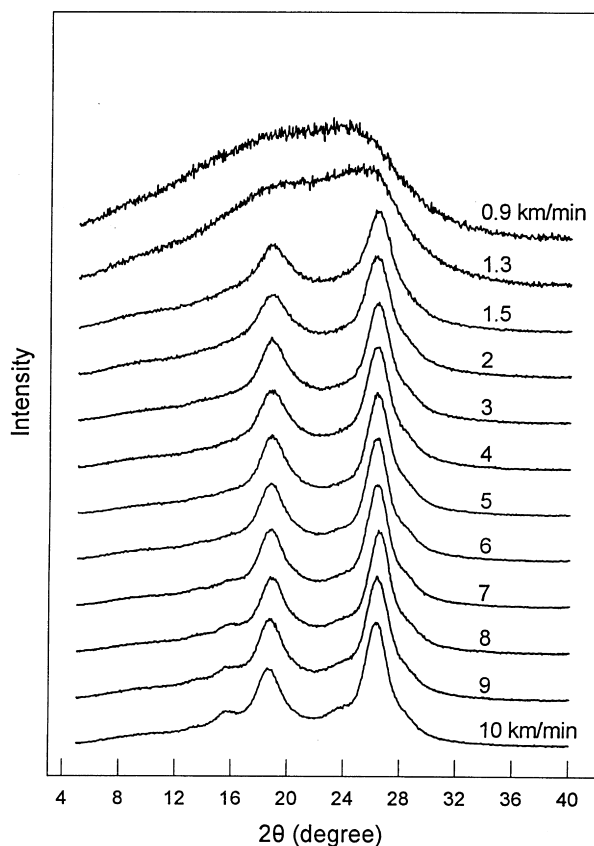


Fig. 3. Equatorial X-ray diffraction profiles of as-spun PEN fibers as a function of take-up velocity.

presented in Fig. 1. The density rises rapidly up to ca 2.5 km/min and then levels off at ca 4 km/min to a value of approximately 1.367 g/cm<sup>3</sup>.

WAXD photographs of PEN fiber samples spun at three take-up velocities are illustrated in Fig. 2. As seen in this figure, at the low take-up speed of 1.3 km/min, no uniform amorphous halo is observed. The intensity of amorphous scattering concentrates toward the equator, indicating an improved orientation of the molecules in the predominantly amorphous sample, although without distinct crystallization. At an intermediate level of take-up speed, i.e. 4 km/min, the indication of some developed crystalline material is evident. This result corresponds well to the relatively high density observed at this speed. The three major diffraction spots apparent are attributed to  $(-1 - 11)$  (020) and (200) reflections of the  $\beta$  form [9], with some weak diffractions of the  $\alpha$  form superposed. The reflections of (010) and (100) of the  $\alpha$  form became stronger at the ultrahigh speed of 10 km/min, indicating that as-spun fiber consists of a mixture of crystals of the oriented  $\alpha$  and  $\beta$  forms. Furthermore, comparing Fig. 2(b) and (c), one observes that the crystalline reflections become sharp along the equator but not along the azimuth with increasing take-up speed, indicative of development of crystalline size but unchanged crystalline orientation.

In Fig. 3, the equatorial WAXD traces are given for as-spun fiber samples prepared at various take-up velocities. One evident effect of take-up speed on the crystalline structure is observed. The filaments taken up at lower speeds reveal only broad unresolved curves. At slightly higher take-up velocity, for example, at 1.5 km/min, a fairly well resolved pattern is found. The reflections from (020) and (200) planes of the  $\beta$  modification crystal are clearly visible at  $2\theta = \text{ca } 18.4$  and  $26.2^\circ$ , respectively. A diffraction peak narrowing with increase of take-up speed is also observed. According to Scherrer's formula, peak width is related to the crystalline size in the direction perpendicular to the crystal plane involved. Therefore, it may be concluded that the lateral dimensions of the crystals in the filaments wound at higher velocities are relatively large, indicative of a well-developed crystalline structure. Further, when the take-up speed was increased to 7 km/min, crystalline reflections of (010) and (100) planes at  $2\theta = \text{ca } 15.5$  and  $23.5^\circ$  have started to appear, which are those from the  $\alpha$  modification [9], indicating that the content of the  $\alpha$  form crystal modification may be promoted by increased take-up velocity. The content ratio of the two crystal modifications,  $\alpha$  and  $\beta$  forms, however, cannot be evaluated because the (200) reflection of the  $\beta$  form and the  $(-110)$  reflection of the  $\alpha$  form overlap in the vicinity of  $2\theta = 26\text{--}27^\circ$ . Further, it is worth noting that the crystalline development starts at noticeably lower take-up speed in this study than it does in those reported by other authors [18,23,24,26,27]. For example, both well-resolved WAXD traces (Fig. 3) and rapid density increases (Fig. 1) were observed when the take-up speed was raised from 0.9 to 2 km/min. In most other published studies [23,24,26,27], such abrupt changes appear in the vicinity of 4 km/min. The reasons for the well-developed crystalline structure and molecular orientation (Fig. 1) achieved at relatively low take-up velocity in this study may be attributed to two factors, a relatively slower cooling rate along the spinline because no cooling chamber was used, and to the molecular weight, which in our case was significantly higher than that reported by others. A gentle cooling condition may allow a longer time and a higher temperature for the crystal growth process to occur in virgin extrudate, while a higher threadline tension intrinsic to the higher molecular weight used might promote stress-induced crystallization. Details will be discussed later.

The structural features of the as-spun fibers were also studied using infrared analysis. Infrared spectra in the range between 3200 and 700 cm<sup>-1</sup> (except for certain regions where no detectable absorption bands appear) are shown in Fig. 4 for three fiber samples spun at 1.3, 4.0 and 10 km/min. Most of the observed bands have been assigned [5]. According to Ref. [5], the bands at 3050, 2990 and 2890 cm<sup>-1</sup> are considered to be related to the CH stretching mode in the naphthalene ring, the bond antisymmetric and symmetric stretching vibrations of CH<sub>2</sub> in the ethylene glycol segment, respectively. The intensity of these bands

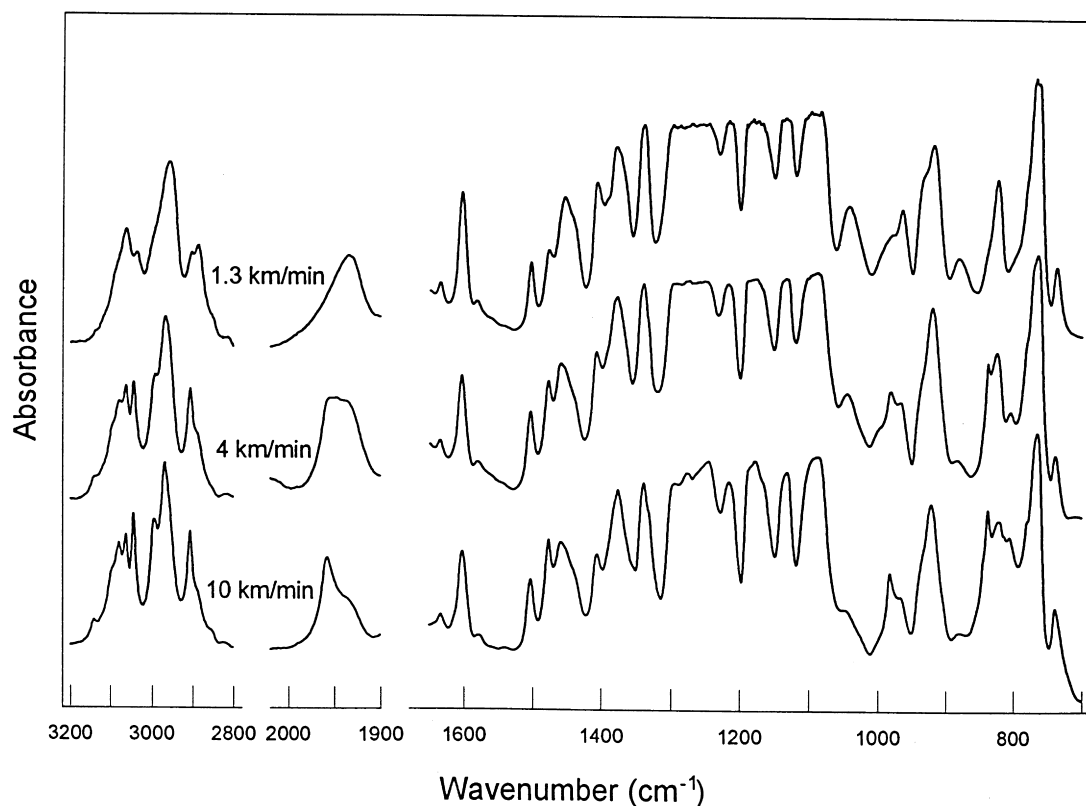


Fig. 4. Infrared spectra of as-spun PEN fibers taken up at the indicated velocity.

increases upon heat treatment and they are accordingly assigned to be crystalline bands. For the bands which reveal dichroic character, 1477, 1337, 835 and 810  $\text{cm}^{-1}$  vibrations and 1450 (it appears at 1460  $\text{cm}^{-1}$  in this study), 1370, 1090 and 1044  $\text{cm}^{-1}$  vibrations, these were considered to be associated with the *trans* and the *gauche* conformations, respectively. As seen in Fig. 4, the intensity of 3050, 2990, 2890, 1477, 835 and 810  $\text{cm}^{-1}$  bands increase significantly with increase in take-up velocity, while bands at 1450 and 1044  $\text{cm}^{-1}$  weaken in intensity in fiber samples wound at higher velocity. These results are indicative of improved crystallinity and molecular orientation achieved in high-speed spun fiber samples. The results are consistent with the observations in birefringence, density and WAXD earlier reported herein. Four bands appearing in Fig. 4, located at ca 1960, 1940, 980 and 880  $\text{cm}^{-1}$  which have not yet been assigned, also reveal a sensitivity for morphological change. With take-up speed increasing from 1.3 to 10 km/min, intensity of the 1940 and 880  $\text{cm}^{-1}$  bands decreases gradually while the others, 1960 and 980  $\text{cm}^{-1}$  bands, increase intensely. As pointed out by Heuvel et al., a primary molecular deformation mechanism of the PET oriented filaments is considered to be the *gauche*–*trans* transition when the filament is elongated. [29,30] Under certain conditions such as fiber being spun at higher speed or being subjected to drawing, the molecules tend to align along the fiber axis by uncoiling, with the result that the amount of *gauche* diminishes and *trans* conformer increases

[29,30]. Such a molecular deformation mechanism is also considered suitable for PEN as-spun fibers, where the as-spun fibers prepared at higher speed should contain more *trans* conformers and less *gauche*. From the experimental results presented above, therefore, bands at 1940 and 880  $\text{cm}^{-1}$  and bands at 1960 and 980  $\text{cm}^{-1}$  are hypothesized to be associated, respectively, with *gauche* and *trans* conformers. Their take-up velocity dependence and the relationship between the relative intensity of these bands and the birefringence data are discussed below.

The detailed infrared spectra, over the wavenumber region 800–1050  $\text{cm}^{-1}$ , of as-spun PEN fibers obtained at various take-up velocities are shown in Fig. 5. The first appearance of the IR bands associating with the *trans* conformers at 810, 835 and 980  $\text{cm}^{-1}$  is observed for fiber wound at 1.5 km/min. This observation corresponds well to the abrupt respective changes in birefringence, density and WAXD scans also observed at this speed. With further velocity increase, the intensity of these same bands increases. In contrast, intensity of IR bands associated with *gauche* conformers at 880 and 1044  $\text{cm}^{-1}$  decreases gradually. The band at 925  $\text{cm}^{-1}$  is assigned to the naphthalene ring vibration [5], hence its magnitude may be used as an internal standard to normalize among samples for variations in mass, as is done in the case of poly(ethylene terephthalate)[31].

Fig. 6 shows the respective changes of infrared absorption ratio  $I_{980}/I_{925}$  and  $I_{880}/I_{925}$  with take-up velocity. A high value of absorption ratio  $I_{880}/I_{925}$  (or low value of  $I_{980}/I_{925}$ ) is

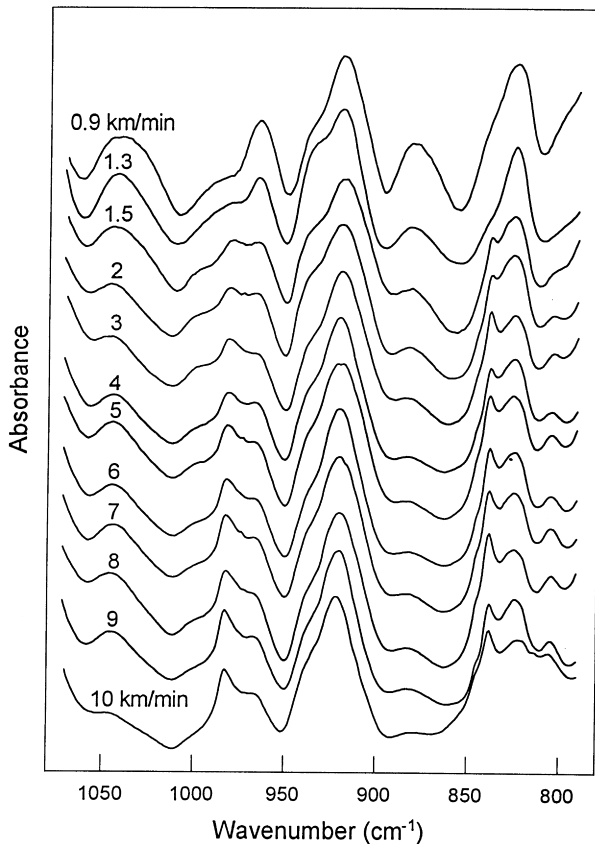


Fig. 5. Detailed infrared spectra (in the wavenumber region of 800–1050  $\text{cm}^{-1}$ ) of as-spun PEN fibers as a function of take-up velocity.

considered indicative of a relatively high percentage of *gauche* conformations being present in a given sample or a relatively high proportion of coiled molecules. From these data, one can see clearly that PEN fiber spun at 0.9 km/min has a high *gauche* conformer content. By comparison with its equatorial WAXD curve (Fig. 3), this sample is characterized by both a low degree of molecular extension and essentially a totally amorphous structure. This results in the observed low birefringence, low density, and poor mechanical properties to be discussed later. Again, a significant increase in *trans* conformer content is observed for samples wound at 1.5 km/min. Following this, one observes a rapid change in the absorption ratio  $I_{980}/I_{925}$  and  $I_{880}/I_{925}$  which next attain the saturated stage in the speed range of 5–10 km/min. As stated above, the change in the absorption ratios is a direct reflection of the percentage of specific conformers. The degree of molecular extension may also be estimated from such changes. The rapid increase of the *trans* conformer in the speed range below 5 km/min, therefore, signifies that the molecular chains were stretched significantly in the direction of the fiber axis. This change conforms very well with the tendency observed for the birefringence of variations in the same speed range.

### 3.2. Threadline tension and how certain factors affect it

As mentioned previously, in the relatively low take-up velocity range, the respective levels of birefringence and density of the instant as-spun PEN fibers are much higher than those reported by other researchers. For example, by way of comparison, the birefringence and density data in this study are, respectively, 0.20 and 1.35  $\text{g}/\text{cm}^3$  for the as-spun fiber wound at 2 km/min, those in other publications

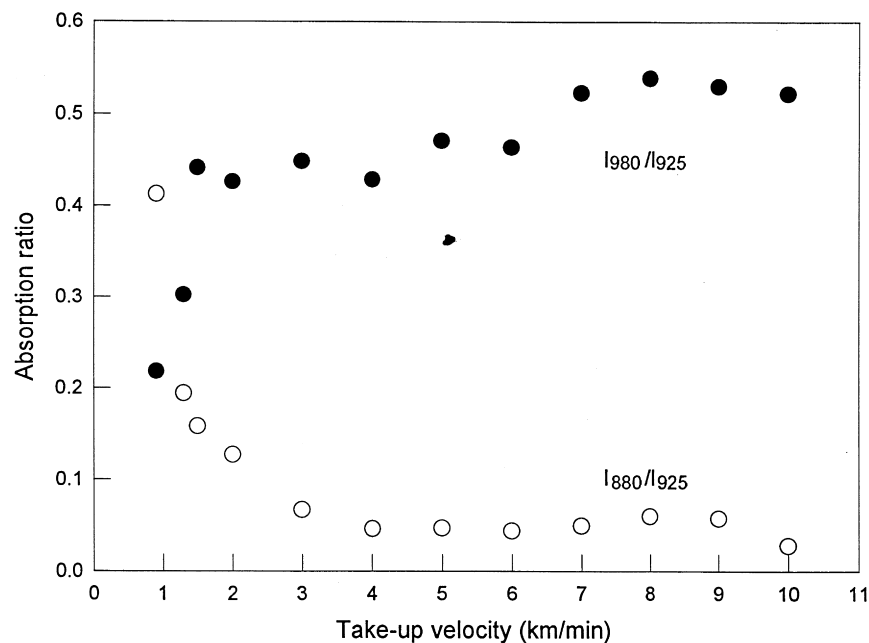


Fig. 6. Plots of absorption ratio for various PEN as-spun fibers.

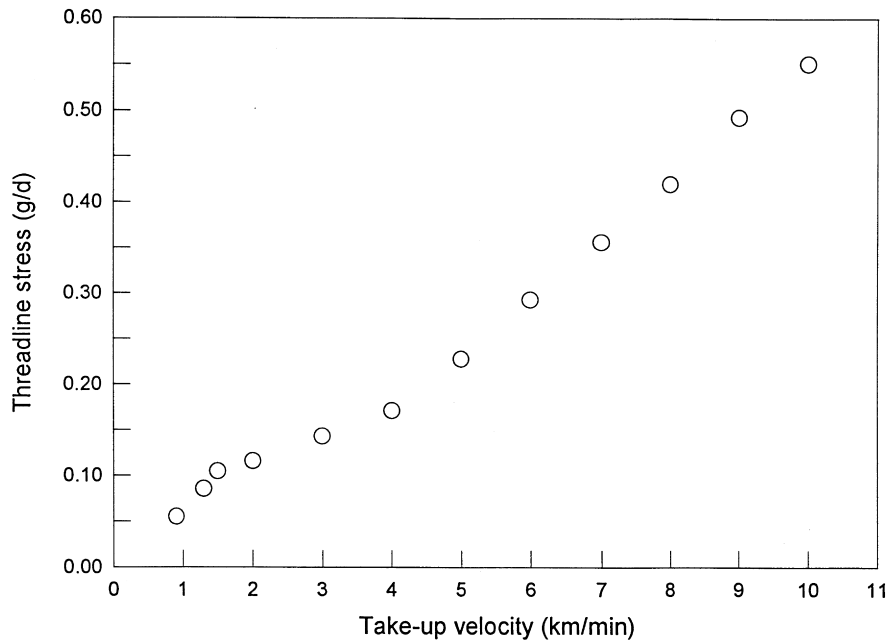


Fig. 7. Threadline stress of as-spun PEN fibers as a function of take-up velocity.

are ca 0.05–0.15 and ca 1.33 g/cm<sup>3</sup> [18,23,24,26,27]. These results mean that the molecular orientation in both amorphous and crystalline phases and crystallization in our samples were significantly developed at quite low take-up speed. In order to understand this phenomenon, the relationship between sample structure and threadline tension was considered.

Threadline tension present in the spinline is responsible for the elongational deformation of molten filament, which in turn induces molecular orientation in the spinline. The

threadline tension is made up primarily of three components, i.e. inertial force due to filament acceleration, frictional force due to air drag, and rheological drag at the spinneret [32]. Among many processing parameters in melt spinning, certain variables such as take-up velocity and spinline length may be strongly related to the inertial and frictional force, respectively. The viscoelastic behavior of the molten extrudate associated with the high-molecular weight of polymer used and the processing temperature may relate to the rheological drag. Finally, these processing

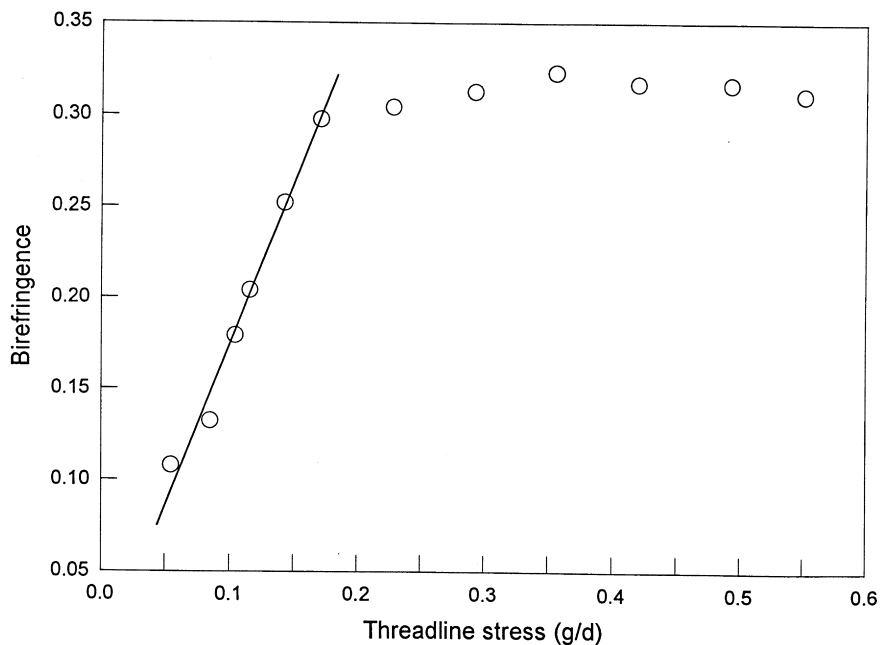


Fig. 8. The birefringence plotted against the threadline stress measured at the solidification point.

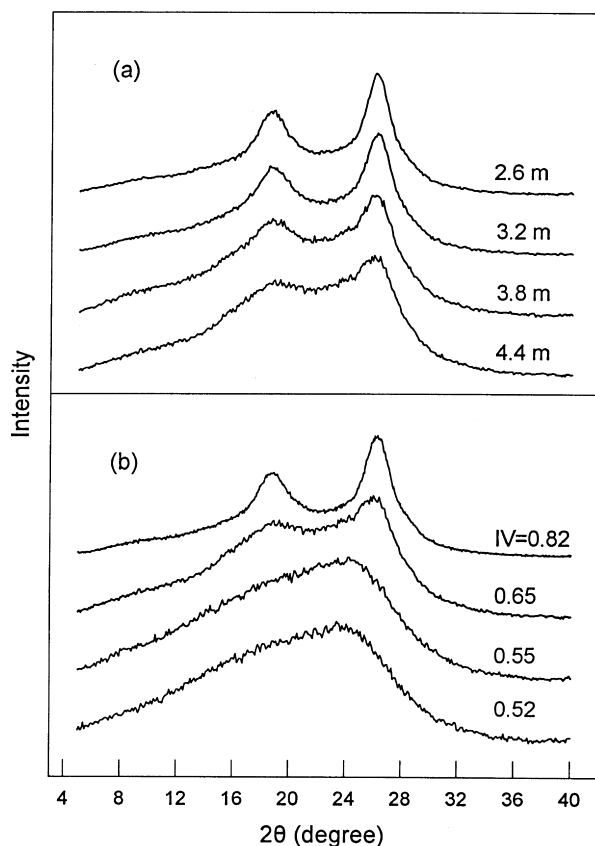


Fig. 9. Equatorial X-ray diffraction profiles of as-spun PEN fibers as a function of: (a) threadline length; and (b) molecular weight of polymer.

parameters may influence the level of threadline tension in a large or small way. The dependence of threadline tension on such variables has been studied in this work.

Fig. 7 plots threadline stress as a function of the take-up velocity. As predicted, the level of threadline stress was gradually increased as take-up speed was increased. The stress increases from ca 0.05–0.55 g/d in the spinning speed range of 0.9–10 km/min. Therefore, improved molecular orientation and higher mechanical properties (to be discussed later) observed in samples wound at higher speeds can be attributed simply to the higher threadline stress.

The birefringence values of various PEN fibers were plotted as a function of the threadline stress in Fig. 8. There is a known relationship between  $\Delta n$  and threadline stress values for melt spun filaments, which may be described by the following equation [23]:

$$\Delta n = C_{\text{opt}} \times \sigma \quad (3)$$

where,  $C_{\text{opt}}$  is the stress optical coefficient, and  $\sigma$  is the threadline stress measured at the freeze point. For PET melt spun filaments, the stress optical coefficients ranging from 0.65 to 0.92 d/g were reported [33]. Iizuka et al. found a  $C_{\text{opt}}$  of 16.1  $\text{GPa}^{-1}$  ( $\sim 1.92$  d/g) for PEN fibers spun at take-up speed range from 1.5 to 5 km/min. Comparing Figs. 7 and 8, there appears to be a linear relationship between the birefringence and the threadline stress data for the as-spun fibers wound in the velocity range below 5 km/min. The line drawn in Fig. 8 permits determination of the stress optical coefficient for these samples. The slope of this line, e.g.  $C_{\text{opt}}$ , is 1.61 d/g. This value agrees fairly well with Iizuka's data, and is much higher than that of PET. From the definition of  $C_{\text{opt}}$  giving by Eq. (3), the higher  $C_{\text{opt}}$  obtained for PEN means that a greater birefringence increase can be achieved under the same threadline stress level, indicating that stress induced molecular orientation is easier in PEN than that in PET. On the other hand, as seen in Fig. 8, samples spun at a higher speed range obviously deviate from the linear relationship. As compared with the data shown in Figs. 1 and 6, it means that increased threadline stress alone can no longer impel the orientation development significantly, when the take-up speed varies from 5 to 10 km/min. However, a noteworthy fact is that the  $\alpha$  form crystalline modification occurs in this higher take-up speed range, although obvious increases of birefringence and mechanical properties (to be discussed later) are not observed. It has been pointed out that the  $\beta$  form crystal in melt spun PEN fibers can be transformed to the  $\alpha$  form by application of high tensile stress. Quantitative analysis of this and related problems is planned for future studies.

The respective influence of spinline length and molecular weight on the threadline tension, morphology and properties of resultant PEN fibers is shown in Fig. 9 and Table 1. All samples were wound at the same take-up speed of 2 km/

Table 1

Preparation conditions, structural analysis and physical properties of various PEN fiber samples

Conditions		Threadline stress (g/d)	$\Delta n$	Density ( $\text{g}/\text{cm}^3$ )	Tenacity (g/d)
Sample IV (dl/g)	Spinline length (m)				
0.65	2.6	0.112	0.1958	1.3502	4.62
0.65	3.2	0.116	0.1983	1.3478	4.69
0.65	3.8	0.098	0.1985	1.3518	4.46
0.65	4.4	0.103	0.1930	1.3476	4.39
0.82	4.4	0.116	0.2035	1.3573	5.19
0.65	4.4	0.103	0.1930	1.3476	4.39
0.55	4.4	0.052	0.1096	1.3396	3.01
0.52	4.4	0.045	0.0749	1.3375	2.19



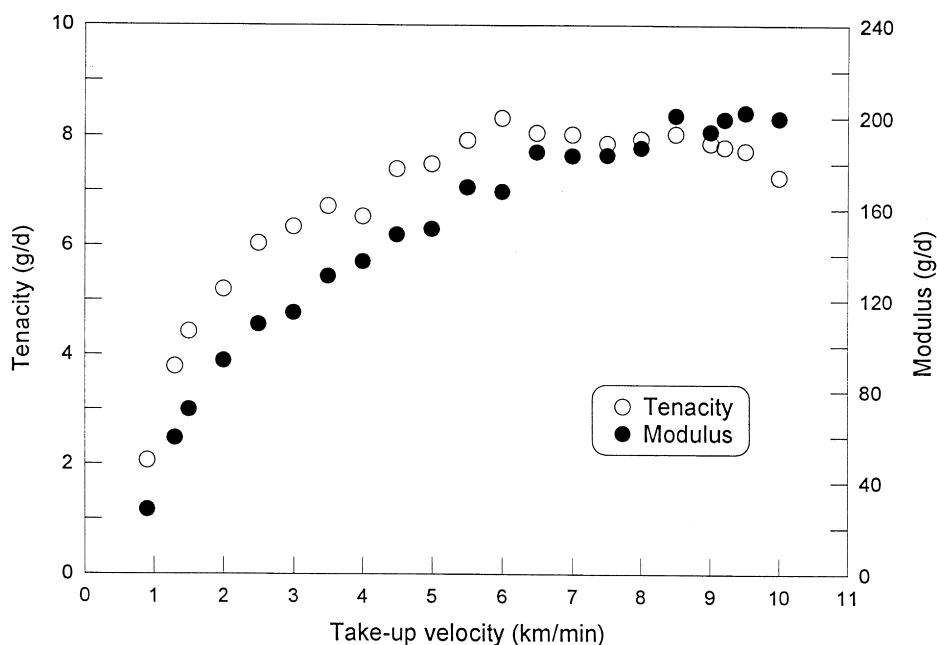


Fig. 10. Tenacity and initial modulus of as-spun PEN fibers as a function of take-up velocity.

min. For one series, spinline length was changed from 4.4 to 2.6 m in 0.6 m intervals, by moving the extruder down toward the godet. For the other series, fiber samples with various molecular weights were prepared by altering spinning temperature and forcing varying degrees of degradation in the extrudate. In the case of high-speed melt spinning of PET filament, Shimizu et al. examined the air drag and the inertial contributions to the spinline stress and structure of resultant PET fibers. Their experiment led to a conclusion that air drag causes a small effect on the fiber structure formation, but the inertial stress plays an important role in its formation [34]. In contrast, it has also been reported that air drag force increases with increasing distance between the spinneret and the take-up godet, and influences importantly fiber structure for the case of fine denier PET filaments [35]. From the data shown in Fig. 9 and Table 1, the influence of spinline length on the morphology and properties appears to be very small. Threadline stress measured for four samples of different spinline length does not exhibit any obvious difference. The shape and intensity of WAXD traces, the birefringence and density values, among the four samples are essentially the same. In contrast, threadline stress measured for a fiber sample having higher molecular weight shows a higher value. The higher molecular weight sample appears to possess more developed orientation and crystallization, resulting in well-resolved X-ray diffraction curves and higher value in  $\Delta n$ , density and, as will be shown, better mechanical properties.

In the experimental and theoretical studies of PET melt spinning, it has been found that in the range of high velocities, the inertial stress related with the winding speed plays a most important role in the formation of fiber structure [34]. In the range of lower velocities, threadline tension is

controlled by the rheological force [32]. The experimental facts described above are considered to conform with these conclusions quite well. In our case of PEN melt spinning performed at various speeds, higher spinning speed generates a higher inertial force, resulting in a significant increase in the threadline tension, and ultimately in high birefringence. On the other hand, at the same take-up speed, the rheological drag is enhanced by the use of high-molecular weight PEN. The enhanced rheological drag also induces an increased threadline tension, which is considered to be an important factor in explaining the well-developed structures formed in fiber samples wound at quite low speed.

### 3.3. Physical properties of fiber samples

The tenacity and initial modulus of as-spun PEN fiber samples were plotted against the take-up velocities in Fig. 10. These results indicate that fiber wound at high speed exhibits significantly improved physical properties. The tenacity and modulus of PEN fibers increase rapidly with increasing speed from 0.9 to 5 km/min. The change in slope occurs at speeds between 5 and 10 km/min. The tenacity levels off in this range, suggesting that highly oriented molecular chains have formed and their level of orientation has reached a saturated state as suggested by Fig. 1. At the highest take-up speed of 10 km/min, the tenacity exhibits a slight decrease. This appears to be somewhat similar to PET behavior, where defects such as microvoids or skin-core structure are formed at ultrahigh spinning speed [36]. The details of this possibility are being studied. On the other hand, the initial modulus of as-spun fiber exhibits a monotonic increase, albeit with decreasing rate at the higher speeds. A progressively improved crystalline structure

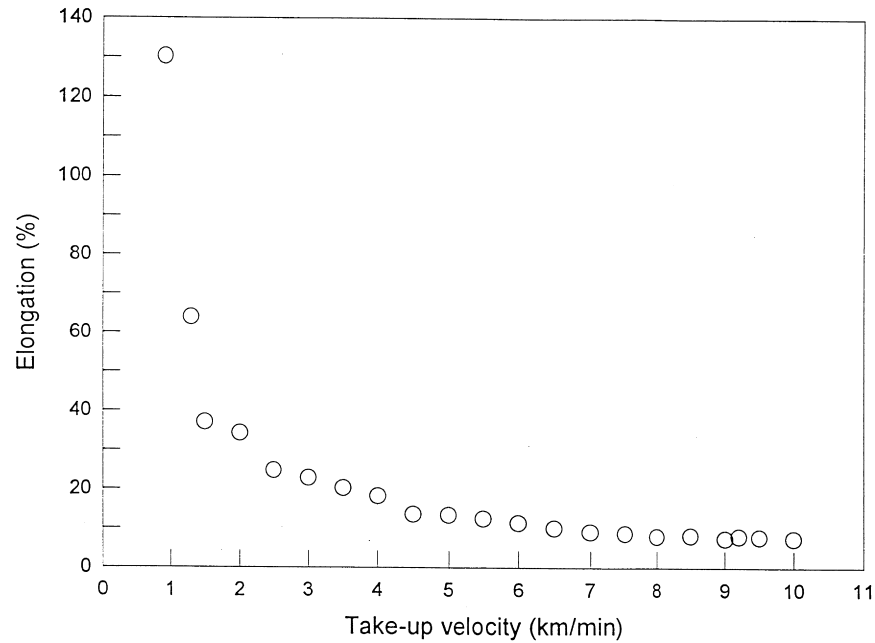


Fig. 11. Elongation to break of as-spun PEN fibers as a function of take-up velocity.

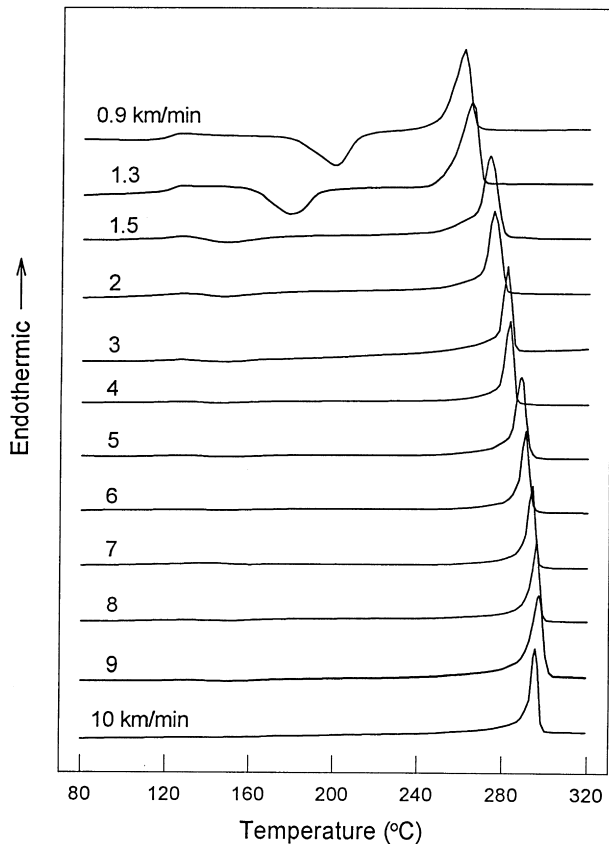


Fig. 12. DSC scans of as-spun PEN fibers taken up at the indicated velocity.

may raise the modulus to its highest value when take-up speed reaches 10 km/min. The highest tenacity of about 8 g/d and the highest modulus of 200 g/d were achieved at the high take-up velocities of 7–10 km/min. These maximum tenacity and modulus values obtained in PEN high-speed as-spun fibers are much higher than those of as-spun PET fibers prepared at the same speed range, where the typical tenacity and modulus are about 4.5 and 100 g/d, respectively [28]. Fig. 11 shows the relationship between elongation to break of as-spun PEN filaments and the take-up speeds. Elongation decreases gradually up to 10 km/min. However, even at intermediate speeds, for example, at 5 km/min, this value has dropped down to about 15%, which is considerably lower than that of PET as-spun fiber wound at the same speed (~70%) [28].

Typical DSC diagrams of PEN as-spun fibers prepared at various take-up speeds are given in Fig. 12. The glass transition is found at a constant temperature of 122°C up to speeds of 3 km/min. For the as-spun fibers wound at lower speeds, the glass transition is followed by the cold crystallization exotherm, and following that a melting endotherm appears. Fig. 12 shows the change in size and location of the cold crystallization exothermic peak in as-spun fibers as a function of spinning speed. Increasing speeds lead to a shift in the cold crystallization peak to lower temperatures and reduce the area of the cold crystallization exothermic peak, which is similar to the phenomenon reported for PET [37]. Increased spinning velocity leads to increased molecular orientation in the spun yarn prior to solidification, which, in turn, results in ease of cold crystallization during the heating process in the DSC measurement. At speeds above 4 km/min, only the melting exotherm is observed. The melting temperatures of as-spun fiber samples are

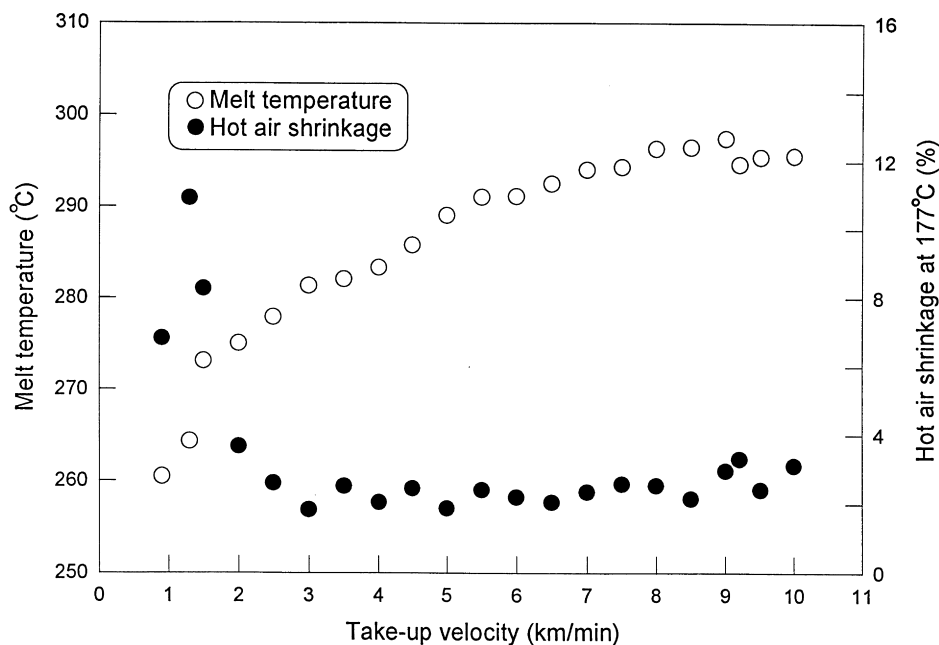


Fig. 13. Plots of melt temperature and hot air shrinkage at 177°C vs. take-up velocity.

plotted against the take-up speed in Fig. 13. The melting temperature is found to increase with increasing take-up speed, starting from ca 260°C for 0.9 km/min spun fiber to 296°C for fiber wound at 10 km/min, suggesting that the crystals become more perfect at higher speed.

Free shrinkage at 177°C of the as-spun fibers as a function of take-up velocity is also shown in Fig. 13. The shrinkage value for fiber spun at 0.9 km/min is relatively low because of its isotropic structure. The shrinkage decreases dramatically as the speeds exceeds 1.5 km/min, and then levels off. This reduction in shrinkage is attributed to the development of significant crystallinity, and consistent with the WAXD traces shown in Fig. 3.

#### 4. Conclusions

High-speed melt spinning of PEN was carried out at various take-up velocities from 0.9 to 10 km/min. The effects of take-up velocity on structure and physical properties of as-spun fibers have been investigated. Generally, high spinning speed induces a high stress along the spinline, resulting in gradual increases in molecular orientation, crystallinity and physical properties. Such improvements in structure and properties are significant in the low-speed range, namely from 0.9 to 4 km/min, and level off in the range of 5–10 km/min, which may be attributed to the saturated state of molecular orientation in this high-speed range.

It was also found that the threadline stress is greatly affected by molecular weight. At take-up speed of 2 km/min, when the measured intrinsic viscosity of extrudate varied from 0.52 to 0.82 dl/g, threadline stress was found to increase from 0.05 to 0.12 g/d, resulting in a significant

increase in birefringence and density, and elevating the tenacity from 2.2 to 5.2 g/d. Based on this observation, the use of and retention of high-molecular weight during processing in this study is considered to be the main reason that our PEN as-spun fibers possess a well-developed molecular orientation, high crystallinity and improved physical properties, including even those fibers prepared at quite low take-up speed.

With the orientation and crystallinity increasing, PEN as-spun fiber with excellent physical properties has been obtained. The tenacity, initial modulus, and elongation to break are, about 8 and 200 g/d and 8%. These values were obtained for take-up velocities of 7–10 km/min.

#### Acknowledgements

The support from Allied Signal Inc. and National Natural Science Foundation of China (grant no. 59873003) was gratefully appreciated. The authors would also like to thank Mr Ferdinand Lundberg for his invaluable assistance during the preparation of the PEN fiber samples.

#### References

- [1] Cook JG, Huggill HPW, Lowe AR. BP 604073, 1948.
- [2] Mencik Z. Chem Prum 1967;17:78.
- [3] Ouchi I, Noda H. Sen-i Gakkaishi 1973;29:P405.
- [4] Hamana I, Fujiwara Y, Kumakawa S. BP 1445464, 1976.
- [5] Ouchi I, Hosoi M, Shimotsuna S. Appl Polym Sci 1977;21:3445.
- [6] Kimura M, Kambe H. Rep Progr Polym Phys Jpn 1979;22:215.
- [7] Cheng SZD, Wunderlich B. Macromolecules 1988;21:789.
- [8] Ghanem AM, Porter RS. Polym Sci Part B: Polym Phys 1989;27:2587.

- [9] Buchner S, Wiswe D, Zachmann HG. *Polymer* 1989;30:480.
- [10] Cakmak M, Wang YD, Simhambhatla M. *Polym Engng Sci* 1990;30:721.
- [11] Ito M, Honda K, Kanamoto T. *Appl Polym Sci* 1992;46:1013.
- [12] Nakamae K, Nishino T, Tada K, Kanamoto T, Ito M. *Polymer* 1993;34:3322.
- [13] Huijts RA, Peters SM. *Polymer* 1994;35:3119.
- [14] Ulcer Y, Cakmak M. *Polymer* 1994;35:5651.
- [15] Murakami S, Nishikawa Y, Tsuji M, Kawaguchi A, Kohjiya S, Cakmak M. *Polymer* 1995;36:291.
- [16] Nakamae K, Nishino T, Gotoh Y. *Polymer* 1995;36:1401.
- [17] Cakmak M, Lee SW. *Polymer* 1995;36:4039.
- [18] Jager J, Juijn JA, van den Heuvel CJM, Huijts RA. *Appl Polym Sci* 1995;57:1429.
- [19] Wang S, Shen D, Qian R. *Appl Polym Sci* 1996;60:1385.
- [20] Ulcer Y, Cakmak M. *Appl Polym Sci* 1996;62:1661.
- [21] Murakami S, Yamakawa M, Tsuji M, Kohjiya S. *Polymer* 1996;37:3945.
- [22] Hill R, Walker EE. *Polym Sci* 1948;3:609.
- [23] Iizuka N, Yabuki K. *Sen-i Gakkaishi* 1995;51:463.
- [24] Nagai A, Murase Y, Kuroda T, Matsui M, Mitsuishi Y, Miyamoto T. *Sen-i Gakkaishi* 1995;51:470.
- [25] Nagai A, Murase Y, Kuroda T, Matsui M, Mitsuishi Y, Miyamoto T. *Sen-i Gakkaishi* 1995;51:478.
- [26] Cakmak M, Kim JC. *Appl Polym Sci* 1997;64:729.
- [27] Miyata K, Kikutani T, Okui N. *Appl Polym Sci* 1997;65:1415.
- [28] Murase Y. *Sen-i Gakkaishi* 1991;47:P564.
- [29] Heuvel HM, Huisman R. *Appl Polym Sci* 1985;30:3069.
- [30] van den Heuvel CJM, Heuvel HM, Faassen WA, Veurink J, Lucas LJ. *Appl Polym Sci* 1993;49:925.
- [31] Kunugi T, Suzuki A, Hashimoto M. *Appl Polym Sci* 1981;26:1951.
- [32] Ziabicki A. *Sen-i Gakkaishi* 1982;38:P409.
- [33] George HH. *Polym Engng Sci* 1982;22:292.
- [34] Shimizu J, Okui N. *Sen-i Gakkaishi* 1983;39:T445.
- [35] Fujimoto K, Iohara K, Ohwaki S, Murase Y. *Sen-i Gakkaishi* 1988;44:477.
- [36] Fujimoto K, Iohara K, Ohwaki S, Murase Y. *Appl Polym Sci* 1991;42:1509.
- [37] Heuvel HM, Huisman R. *Appl Polym Sci* 1978;22:2229.